

Singularity-matching peaks in a superconducting single-electron transistor

Y. Nakamura

NEC Fundamental Research Laboratories, Tsukuba, Ibaraki 305, Japan

A. N. Korotkov

*NEC Fundamental Research Laboratories, Tsukuba, Ibaraki 305, Japan
and Nuclear Physics Institute, Moscow State University, Moscow 119899 GSP, Russia*

C. D. Chen and J. S. Tsai

NEC Fundamental Research Laboratories, Tsukuba, Ibaraki 305, Japan

(Received 18 April 1997)

We report the experimental observation of the recently predicted peaks on the I - V curve of a superconducting single-electron transistor at relatively high temperatures. The peaks are due to the matching of singularities in the quasiparticle density of states in two electrodes of a tunnel junction. The energy shift due to Coulomb blockade provides the matching at finite voltage. [S0163-1829(97)01434-3]

Single-electron effects¹ in superconducting structures have several additional features^{1,2} in comparison with those in normal metals or semiconductors. The main differences are due to the specific role of the parity of the electron number on a small island,^{3,4} the effects of Josephson coupling,^{1,2,5-8} and the specific shape of the quasiparticle density of states (QDS). The last topic has received relatively little attention so far in both theoretical and experimental single electronics, although QDS leads to various interesting effects. Besides the well-known shift of the Coulomb blockade threshold by $4\Delta/e$ in an SSS single-electron transistor (SET) (by $2\Delta/e$ in NSN or SNS cases), let us mention the direct reproduction of the QDS on the I - V curve of the SET with the discrete energy spectrum of the central electrode⁹ and in the case of odd-parity current,¹⁰ singularity-matching (SM) peaks at finite temperatures,¹¹ the limitation of the differential conductance by quantum resistance,^{11,12} and the conductance jump at $V=4\Delta/e$ due to cotunneling.¹²

In this paper we discuss the theory of SM peaks in more detail and report their experimental observation in the SSS SET. Somewhat similar experimental results will be presented soon by another group.¹³

The origin of SM peaks can be easily understood from the ‘‘orthodox’’ theory of the SET.^{1,14} Let us neglect the effects due to Josephson coupling and consider only quasiparticle tunneling. The dc current I through the SET consisting of two tunnel junctions in series can be calculated from the equations^{1,14}

$$I = e \sum_n [\Gamma_1^+(n) - \Gamma_1^-(n)] \sigma(n), \quad (1)$$

$$\sigma(n) [\Gamma_1^+(n) + \Gamma_2^-(n)] = \sigma(n+1) [\Gamma_1^-(n+1) + \Gamma_2^+(n+1)], \quad (2)$$

where $\Gamma_i^\pm(n)$ are the rates of tunneling through i th junction ($i=1,2$) in the positive (+) or negative (-) direction when n extra electrons are present on the central electrode of the

SET, and $\sigma(n)$ is the probability of the charge state n . In the case of the SS junction the tunneling rates $\Gamma_i^\pm(n) \equiv \Gamma_i[W_i^\pm(n)]$ are given by

$$\Gamma_i(W) = \frac{1}{e^2 R_i} \int_{-\infty}^{+\infty} \rho(\varepsilon) f(\varepsilon) \rho(\varepsilon + W) [1 - f(\varepsilon + W)] d\varepsilon, \quad (3)$$

$$\rho(\varepsilon) = \sqrt{\frac{\varepsilon^2}{\varepsilon^2 - \Delta(T)^2}} \theta(\varepsilon^2 - \Delta^2), \quad (4)$$

where $\rho(\varepsilon)$ is the normalized QDS, $\Delta(T)$ is the superconducting energy gap, $\theta(x)$ is the step function, $f(\varepsilon) = 1/[1 + \exp(\varepsilon/T)]$ is the Fermi function, T is temperature, R_i is the normal tunnel resistance of i th junction, and the energy gain W is given by¹⁴

$$W_i^\pm(n) = \frac{e^2}{C_\Sigma} \left[\pm \frac{VC_1 C_2}{eC_i} - \frac{1}{2} \pm (-1)^i \left(n + \frac{Q_0}{e} \right) \right]. \quad (5)$$

Here C_1 and C_2 are the junction capacitances, $C_\Sigma = C_1 + C_2$ is the total island capacitance, and Q_0 is the total background charge which accounts for the initial background charge Q_{00} and the charge induced by the gate voltage V_g , $Q_0 = Q_{00} + V_g C_g$ (for definiteness we consider the gate capacitance C_g as being added to C_1 , although an arbitrary distribution of C_g between C_1 and C_2 is possible in calculations¹⁵).

At low temperatures the quasiparticle current in SSS SET appears only above the voltage threshold

$$V_i = \min_{i,n} [V_{i,n}^{\text{QP}} | V_i > 4\Delta(T)], \quad (6)$$

$$V_{i,n}^{\text{QP}} = \frac{eC_i}{C_1 C_2} \left[\frac{2\Delta(T)C_\Sigma}{e^2} + \frac{1}{2} - (-1)^i \left(n + \frac{Q_0}{e} \right) \right]. \quad (7)$$

[The last equation is the condition $W_i^+(n) = 2\Delta(T)$.]

At temperatures T comparable to the critical temperature T_c , the concentration of the thermally excited quasiparticles

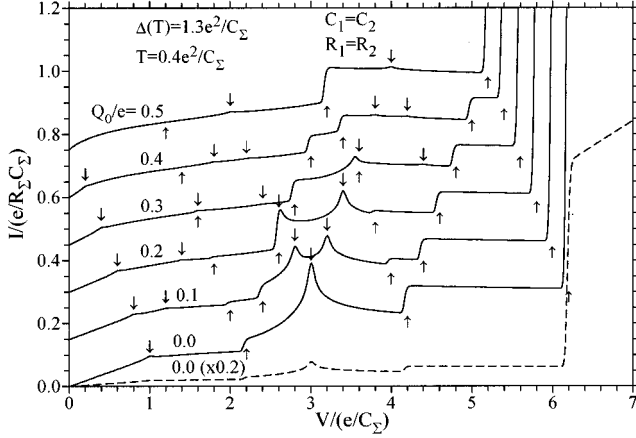


FIG. 1. Theoretical I - V curves of the symmetrical SSS SET with $\Delta(T) = 1.3e^2/C_\Sigma$, $T = 0.4e^2/C_\Sigma$ at $V < V_t$ for several Q_0 taking into account only quasiparticle tunneling. Notice the presence of SM peaks (marked by down arrows) and steps (up arrows). A small phenomenological smearing $w = 0.01\Delta(T)$ of the superconducting gap is assumed. Curves are shifted vertically for clarity.

becomes considerable, and this modifies the shape of the I - V curve, in particular, creating several additional features at $V < V_t$. As an example, Fig. 1 shows the theoretical I - V curve of the symmetrical SET transistor with $\Delta(T) = 1.3e^2/C_\Sigma$, $T = 0.4e^2/C_\Sigma$ for several values of Q_0 [the relatively large ratio of $\Delta(T)/(e^2/C_\Sigma)$ is chosen to show more features]. One can see two types of features: peaks (marked by down arrows) and steps (up arrows).

The peaks positions constitute two series:¹¹

$$V_{i,n}^{\text{SM}} = \frac{eC_i}{C_1C_2} \left[\frac{1}{2} - (-1)^i \left(n + \frac{Q_0}{e} \right) \right], \quad (8)$$

which correspond to the condition $W_i^+(n) = 0$ [obviously, the condition $W_i^-(n) = 0$ gives the same set of voltages]. For such tunneling with zero energy gain the singularities of the density of states of two electrodes match [recall that we consider the same $\Delta(T)$ in all electrodes], that leads to the increase of the tunneling rate $\Gamma_i^+(n)$ and explains the name of SM peaks. In BCS theory $\Gamma_i^+(n)$ is formally infinite at $W_i^+(n) = 0$ (logarithmic divergence). Although the current through the SET transistor remains finite being governed by the stationary master equation (2), the divergence of Γ would lead to a very high and narrow center of the SM peak. To take into account the inevitable smoothing of the singularity of $\rho(\epsilon)$, in Fig. 1 we assumed (phenomenologically) a small Gaussian inhomogeneous broadening of $\Delta(T)$ with dispersion $w = 0.01\Delta(T)$. The peak height depends very weakly (logarithmically) on w provided $w \ll \Delta(T)$.

The origin of SM peaks is similar to that of well-known peaks² on the I - V curve of a single junction with different energy gaps $\Delta_1(T)$ and $\Delta_2(T)$ of electrodes at $V = [\Delta_1(T) - \Delta_2(T)]/e$. In our case the energy gaps can be the same, and the energy shift is provided by the Coulomb blockade. However, this analogy is not complete. For example, in our case both singularities match simultaneously. Another differ-

ence is that the reverse process (tunneling back) also has a large rate, and the net transport is due to tunneling through the other junction.

The voltage position of SM peaks coincides with the position of the recently observed peaks¹⁰ in the SSS SET at low temperatures when the parity-dependent current is due to the single quasiparticle created by the preceding tunneling event. Notice that the SM peaks are located at the same voltages as the I - V curve cusps (conductance changes) in the normal SET.

At not too high temperatures the SM peaks are more pronounced within the voltage interval $2\Delta(T)/e < V < 2\Delta(T)/e + e/C_\Sigma$ (see Fig. 1). The lower bound is the condition that the tunneling through the other junction which restores the system into the initial charge state and gives the contribution to the net current, is sufficiently fast, $W = eV > 2\Delta(T)$. The upper bound is the condition that after this restoring the tunneling of the next electron through the same junction (which drives the system out of ‘‘resonance’’) has a small rate, $W = eV - e^2/C_\Sigma < 2\Delta(T)$. Hence, not more than two closely located peaks from the series given by Eq. (8) can be well pronounced on the I - V curve.

The important property of SM peaks is their specific temperature dependence. They should be absent at small T (because there are no thermally excited quasiparticles), and their height grows with T for some temperature range [see Fig. 3(b) below] until they begin to decrease due to the suppression of superconductivity and/or correlation between tunneling events. Notice that the voltage position of the SM peaks does not change with temperature despite the dependence $\Delta(T)$.

One can see from Fig. 1 that the SM peaks are rather broad and have an asymmetric shape so that they have longer and higher tails on the higher-voltage side. When the peak is not well pronounced, this tail resembles a plateau. When the SM feature is even weaker, it is seen as a small kink on the I - V curve (Fig. 1).

The other features seen in Fig. 1 are the step structures in the I - V curve which are similar to the step at $V = V_t$. Their positions satisfy the same condition $W_i^+(n) = 2\Delta(T)$ and hence, the same Eq. (7) as for V_t . So the position of these two series of steps on the V - Q_0 plane is just a continuation of the straight lines corresponding to V_t (they exist both above and below V_t). The steps in Fig. 1 are smoothed because of a finite w .

Notice that while the steps corresponding to Eq. (7) are usually positive (increase of the current), they can also be negative—for example, when the step position is on the negative slope of a SM peak (the decrease of the current occurs because the charge state having the resonant tunneling rate becomes less probable).

Besides the steps described by Eq. (7), at relatively high temperatures the theory predicts an appearance of very small negative steps (both below and above V_t) at

$$V_{i,n}^{\text{NS}} = \frac{eC_i}{C_1C_2} \left[-\frac{2\Delta(T)C_\Sigma}{e^2} + \frac{1}{2} - (-1)^i \left(n + \frac{Q_0}{e} \right) \right], \quad (9)$$

that corresponds to the condition $W_i^+(n) = -2\Delta(T)$. The steps are negative because the dependence $\Gamma(W)$ given by Eq. (3) has a step down at $W = -2\Delta(T)$. The effect is very weak because of the factor $\exp[-4\Delta(T)/T]$ and also because of the existence of the opposite effect due to the simulta-

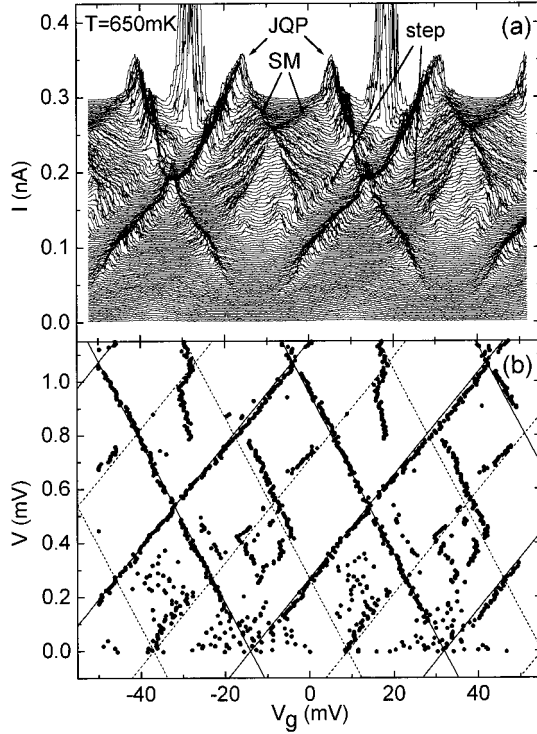


FIG. 2. (a) The experimental dependence of the current I on the gate voltage V_g for SSS SET at $T=650$ mK. The bias voltages V range from 0 to 0.828 mV with a step of $7.08 \mu\text{V}$. The curves are shifted vertically by $\Delta I(\text{pA})=281 \times V(\text{mV})$. (b) The positions of the current maxima on the V - V_g plane. The solid lines fit JQP peaks. The dashed lines show theoretical positions of SM peaks.

neous threshold condition $W_i^- [n - (-1)^i] = 2\Delta(T)$ (negative steps have not been observed in our experiment).

The aluminum-based single-electron transistors were fabricated using the standard two-angle evaporation technique. The details of the fabrication are given in Ref. 16. Figure 2(a) shows the experimental dependence of the current on the gate voltage for different bias voltages at $T=650$ mK. The largest feature seen in the figure is the onset of the fast quasi-particle tunneling at $V > V_t$ [Eq. (6)]. [Actually, we see peaks because of the small current scale of the Fig. 2(a); for larger bias voltages they transform into plateaus with sufficiently sharp edges.] The well-pronounced peaks along the straight lines intersecting the abscissa axis at $V_g = -14$ mV and $V_g = 32$ mV are the so-called JQP (Josephson-plus-quasiparticle cycle) peaks.⁵ [They are due to Josephson coupling and, hence, are outside of the scope of the present paper. The position of JQP peaks is given^{5,6,16} by Eq. (8) without the term $\frac{1}{2}$ inside parentheses.] The step structures can be seen along the lines [see Eq. (7)] which are the continuation of the main threshold $V_t(V_g)$ [they start from the large features due to V_t in the upper part of Fig. 2(a)]. And finally, the SM peaks are represented as rather broad features along the straight lines approximately in the middle (theoretically, exactly in the middle) between JQP lines which intersect the abscissa axis roughly at $V_g \approx 10$ mV and $V_g \approx -40$ mV. Small SM peaks have been observed even above V_t . The SM features along the line with negative slope are more pronounced than along the line with positive slope possibly because of the difference in junction resis-

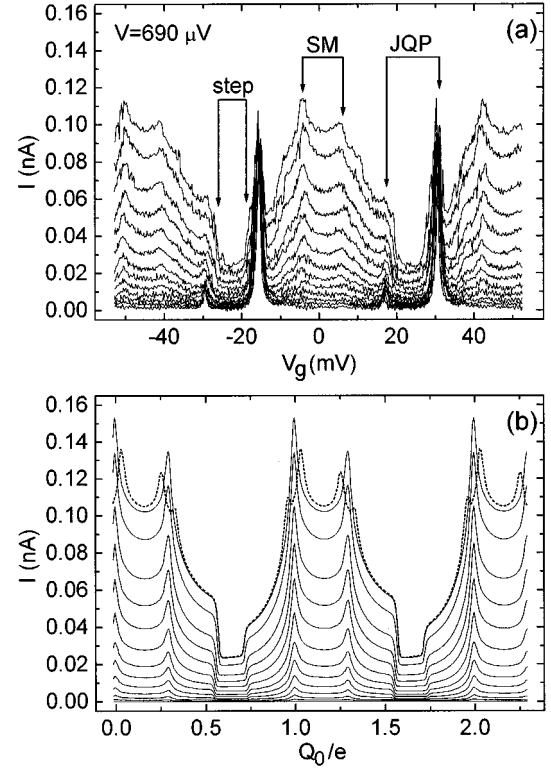


FIG. 3. (a) Experimental I - V_g curves for $V=0.69$ mV at different temperatures which show two SM peaks (and also two JQP peaks and two steps) per period. The temperatures in mK (from top to bottom) are 712, 684, 640, 605, 571, 532, 495, 462, 426, 386, 345, 303, 97. Notice that the height of SM peaks and steps grows with temperature. (b) Solid lines show the corresponding theoretical prediction without fitting parameters. The JQP peaks have not been included in simulations. A small smearing $w=0.03\Delta(0)$ is assumed. Dashed line illustrates the peak splitting due to different $\Delta(T)$ in the island and leads ($\pm 10 \mu\text{eV}$ difference is used).

tances. Similar measurements made at $T=50$ mK do not show SM features as well as additional step structures while JQP peaks remain well pronounced at $V \geq 0.65$ mV.

Figure 2(b) shows the numerically determined positions of the maxima of the I - V_g curves from Fig. 2(a) on the V - V_g plane. From the straight lines corresponding to JQP peaks (solid lines) we determine the junction capacitances $C_1 = 183 \pm 4$ aF, $C_2 = 117 \pm 3$ aF. The gate capacitance $C_g = 3.5$ aF which determines the gate voltage period of 46 mV is included in C_1 because V_g has been measured from the outer side of C_1 . Notice that the bias voltage corresponding to the intersection of two JQP lines directly gives the charging energy $e/C_\Sigma = 0.53$ mV. The minimal V_t of 0.80 mV is used to determine the superconducting gap $\Delta(T) = 0.20$ meV [minimal V_t corresponds to the edge of the almost vertical curved lines in the upper part of Fig. 2(b)].

Dashed lines in Fig. 2(b) show the theoretical position $V_{i,n}^{\text{SM}}$ of SM peaks calculated from Eq. (8). We see that experimental peaks are located at somewhat higher bias voltages. This can be explained in several ways. First, the SM feature has a rather smooth shape, and hence, the addition of any current component which increases with bias voltage leads to the apparent shift of the maximum to higher voltages [we also checked numerically that a relatively large inhom-

geneous broadening of $\Delta(T)$ leads to a similar shift]. Second, the additional contribution to the position shift in Fig. 2(b) can occur because the peaks are determined as the maximum current point over V_g , not over V . (The V_g change which decreases $V_{i,n}^{\text{SM}}$ also weakens Coulomb blockade in the same junction, hence increasing the “background” current and leading to the apparent shift of the maximum position.) Finally, the third possible explanation of the shift (which we believe is most likely) is due to the difference between $\Delta(T)$ in the island and leads. Then each SM peak should split in two [there is some experimental evidence of such a splitting which is slightly seen in Fig. 2(a) and Fig. 3(a)]. Numerical simulations show that the peak corresponding to higher bias voltage is more pronounced [see Fig. 3(b)] while the lower peak is possibly too small to be represented in Fig. 2(b). A difference of about 0.02 meV between the energy gaps would be sufficient to explain the experimental deviation.

The experimental temperature dependence of the SM peaks on I - V_g curves is shown in Fig. 3(a). Besides two SM peaks per period of V_g one can see two steps and two JQP peaks (the heights of JQP peaks are different because the Josephson coupling in one junction has been suppressed¹⁷). We see that SM peaks as well as steps grow with temperature. Solid lines in Fig. 3(b) show the corresponding theoretical I - Q_0 curves calculated without fitting parameters (JQP peaks are not included in the model). The total resistance $R_\Sigma = 605 \text{ k}\Omega$ is obtained from the I - V curve and $R_1/R_2 = C_2/C_1$ is assumed. The gap $\Delta(0) = 0.207 \text{ meV}$ is used to get $\Delta(T) = 0.2 \text{ mV}$ at $T = 650 \text{ mK}$. A small broadening $w = 0.03\Delta(0)$ of the gap was used to eliminate the unphysical divergence of Γ at the peak center, while we did not attempt to fit the experimental SM peak height by w [larger w de-

creases the height, though the dependence is quite weak for $w \leq 0.05\Delta(T)$]. The good correspondence between Figs. 3(a) and 3(b) is an additional proof that the observed peaks are really SM peaks. The dashed curve (corresponding to the top solid curve) illustrates the peak splitting due to different $\Delta(T)$ in the island and leads (a difference of $20 \mu\text{eV}$ is used). One can see that this assumption not only explains the peak position shift and traces of such a splitting in experiment, but also improves the agreement for the peak height.

Let us mention that the height of thermally activated JQP peak (at $V < 2\Delta/e + e/2C_\Sigma$) as a function of V (V_g is varied correspondingly) should also exhibit the SM feature at $V = e/2C_\Sigma$ because at this voltage the tunneling of the second quasiparticle in the JQP cycle is at resonance. There are some traces of such an increase in Fig. 2(a) and also one can see qualitatively that in Fig. 2(a) the JQP peaks start to decrease crudely at $V < e/2C_\Sigma$ (because of the thermal broadening of the SM feature, this smooth boundary moves to lower voltages by $\delta V \approx TC_\Sigma/C_i \approx 0.1 \text{ mV}$). Similar behavior should be expected for the height of thermally activated steps with SM feature at $V = 2\Delta(T)$.

In conclusion, we observed SM peaks on the I - V_g dependence of SSS SET at temperatures comparable to T_c . The shape and position of the features agree well with the theoretical prediction.

We thank the group from the University of Jyväskylä for the information about their experimental results¹³ prior to publication. The work was partially performed under the management of FED as a part of the MITI Research and Development Program Superconducting Electron Devices Project supported by NEDO.

¹D. V. Averin and K. K. Likharev, in *Mesoscopic Phenomena in Solids*, edited by B. L. Altshuler *et al.* (Elsevier, Amsterdam, 1991), p. 173.

²M. Tinkham, *Introduction to Superconductivity* (McGraw-Hill, New York, 1996).

³D. V. Averin and Yu. V. Nazarov, *Phys. Rev. Lett.* **69**, 1993 (1992).

⁴M. T. Tuominen, J. M. Hergenrother, T. S. Tighe, and M. Tinkham, *Phys. Rev. Lett.* **69**, 1997 (1992).

⁵T. A. Fulton, P. L. Gammel, D. J. Bishop, and L. N. Dunkleberger, *Phys. Rev. Lett.* **63**, 1307 (1989).

⁶D. V. Averin and V. Y. Aleshkin, *JETP Lett.* **50**, 367 (1989).

⁷L. J. Geerligs, V. F. Anderegg, J. Romijn, and J. E. Mooij, *Phys. Rev. Lett.* **65**, 377 (1990).

⁸P. Joyez, P. Lafarge, A. Filipe, D. Esteve, and M. H. Devoret, *Phys. Rev. Lett.* **72**, 2458 (1994).

⁹D. C. Ralph, C. T. Black, and M. Tinkham, *Phys. Rev. Lett.* **74**, 3241 (1995).

¹⁰Y. Nakamura, C. D. Chen, and J. S. Tsai, *Czech. J. Phys.* **46**, 3339 (1996).

¹¹A. N. Korotkov, *Appl. Phys. Lett.* **69**, 2593 (1996).

¹²D. V. Averin, A. N. Korotkov, A. J. Manninen, and J. P. Pekola, *Phys. Rev. Lett.* **78**, 4821 (1997).

¹³A. J. Manninen, Yu. A. Pashkin, A. N. Korotkov, and J. P. Pekola, *Europhys. Lett.* (to be published).

¹⁴K. K. Likharev, *IEEE Trans. Magn.* **23**, 1142 (1987).

¹⁵A. N. Korotkov, R. H. Chen, and K. K. Likharev, *J. Appl. Phys.* **78**, 2520 (1995).

¹⁶Y. Nakamura, T. Sakamoto, and J. S. Tsai, *Jpn. J. Appl. Phys.* **34**, 4562 (1995).

¹⁷Y. Nakamura, C. D. Chen, and J. S. Tsai, *Phys. Rev. B* **53**, 8234 (1996).